



Adsorption of methylene blue and methyl orange from aqueous solution by iron oxide-coated zeolite in fixed bed column: predicted curves

Lei Zhao^{a,b}, Weihua Zou^b, Lina Zou^a, Xiaotian He^a, Jiyun Song^a, Runping Han^{a,*}

^aDepartment of Chemistry, Zhengzhou University, Zhengzhou, 450001, PR China
Tel. +86 371 67781757; email: rphan67@zzu.edu.cn

^bSchool of Chemical and Energy Engineering, Zhengzhou University, Zhengzhou, 450001, China

Received 21 January 2010; Accepted 1 April 2010

ABSTRACT

Fixed bed column study were carried out to investigate the performance of iron oxide-coated zeolite (IOCZ) in removal of methylene blue (MB) and methyl orange (MO) from aqueous solution in single dye system. The effects of various experimental conditions, such as the flow rate, initial metal concentration and bed depth were studied. The Thomas model, Modified-dose-response model (MDR) and the bed depth service time (BDST) model were used to fit the experimental data. The results were that MDR model was better for the description of breakthrough curves at all experimental conditions than Thomas model. BDST model was applied to predict the service times with various flow rate and initial concentration. IOCZ can be used to remove dyes from solution.

Keywords: Iron oxide-coated zeolite (IOCZ); Adsorption; Methylene blue; Methyl orange; Column

1. Introduction

Wastewaters containing dye may be toxic and even carcinogenic, because most of which are difficult to be decolorized or degraded due to their complex structure and synthetic origin [1]. Industries such as textile, leather, paper, plastics, etc., are some of the sources for dye effluents. The effluents of these industries are highly colored and disposal of these wastes into the environment can be extremely deleterious. Various traditional treatment technologies, such as chemical precipitation, filtration, ion exchange, adsorption on activated carbon and biological methods, are widely applied and have been developed [2,3]. These methods, however, display one or more limitations, such as expensive, generation of secondary pollution and narrow appliance range. To overcome these

limitations, researchers have devoted to search for effective, economic and easily implemented materials [4–6].

It has been demonstrated that iron, aluminum and manganese oxide can removal heavy metal ions and dye from aqueous waste effectively, for their large surface area and high charge density [7,8]. However, the fine particle size of the metal oxides makes it very difficult to separate from the water phase, which limits its application in wastewater treatment. But iron oxide coated-media surface can solve this problem and may be a promising composite for wastewater treatment [9–11]. Zeolite is an ideal natural adsorbent with certain sorption and ion-exchange capability for its special frame structure and often used to remove pollutants and metals from solution [12–16]. Although it has many advantages such as low cost, simple operation and no secondary pollution, modifications are needed to improve its removal performance in wastewater treatment. The zeolite coated with

*Corresponding author.

a layer of iron oxide can not only overcome their respective shortcomings, but also enhance sorption capacity because of bigger surface area and stronger ion exchange capacity [17]. The batch adsorption of methylene blue and methyl orange were studied by the adsorbent and the capacity of adsorption from iron coated zeolite was larger than from zeolite [18,19]. But the dye adsorption by iron coated materials in column was not studied.

This study was designed to test the fixed bed column performance of a medium, iron oxide-coated zeolite (IOCZ), as an adsorbent for the removal of methylene blue (MB, cation dye) and methyl orange (MO, anion dye) from single dye solution in a continuous flow system. The effects of flow rate, influent concentration, and bed height on MB and MO adsorption onto IOCZ were investigated. The dynamic process of adsorption was modeled or analyzed by Thomas model, modified-dose response and BDST model.

1.1. Thomas model

The expression of Thomas model for an adsorption column is given as follows [20]:

$$\frac{C_t}{C_0} = \frac{1}{1 + \exp(k_{Th}q_0m / Q - k_{Th}C_0t)} \quad (1)$$

where, C_t is the effluent dye concentration (mg l^{-1}), C_0 is the influent dye concentration (mg l^{-1}), k_{Th} is the Thomas rate constant (ml (min mg)^{-1}), q_0 is the equilibrium dye uptake per g of the adsorbent (mg g^{-1}), m is the amount of adsorbent in the column (g), Q , the flow rate (ml min^{-1}). The value of C_t/C_0 is the ratio of effluent and influent each dye concentrations. The value of t is breakthrough time (min, $t = V_{\text{eff}}/Q$, V_{eff} is the volume of effluent solution).

The values of k_{Th} and q_0 can be determined from a plot of C_t/C_0 against t using nonlinear regression analysis as the values of C_t/C_0 is within 0.05~0.95.

1.2. Modified dose-response (MDR) model

The modified dose-response model (MDR) [21] is also used to describe column adsorption data. Yan and his coworkers observed that use of this model minimizes the error resulting from the use of the Thomas model, especially at lower or higher time periods of the breakthrough curve. The expression is given as:

$$\frac{C_t}{C_0} = 1 - \frac{1}{1 + \left(\frac{Qt}{b}\right)^a} \quad (2)$$

where a and b are the constants of MDR model, Q is the flow rate.

From value of b , the value of q_0 can be estimated using following equation [21]:

$$q_0 = \frac{bC_0}{X} \quad (3)$$

where, X is the total dry weight of IOCZ in column (g).

1.3. The bed-depth/service time analysis (BDST) model

The BDST model describes a relation between the service time and the packed-bed depth of the column and is expressed as [22]:

$$t = \frac{N_0}{C_0F} Z - \frac{1}{K_a C_0} \ln\left(\frac{C_0}{C_t} - 1\right) \quad (4)$$

where F , the influent linear velocity (cm min^{-1}), N_0 , the adsorption capacity (mg l^{-1}), K_a the rate constant in BDST model (l (mg min)^{-1}), t the time (min) and Z is the bed depth of column (cm).

A plot of t versus bed depth, Z , should yield a straight line where N_0 and K_a , the adsorption capacity and rate constant, respectively, can be evaluated.

A simplified form of the BDST model is:

$$t = aZ - b \quad (5)$$

where

$$a = \frac{N_0}{C_0F} \quad (6)$$

$$b = \frac{1}{K_a C_0} \ln\left(\frac{C_0}{C_t} - 1\right) \quad (7)$$

The slope constant for a different flow rate can be directly calculated by Eq. (8)

$$a' = a \frac{F}{F'} = a \frac{Q}{Q'} \quad (8)$$

where, a and F are the old slope and influent linear velocity, respectively, and a' and F' are the new slope and influent linear velocity. As the column used in experiment has the same diameter, the ratio of original (F) to the new influent linear velocity (F') and original flow rate (Q) to the new flow rate (Q') is equal. For other influent concentrations, the desired equation is given by a new slope, and a new intercept given by:

$$a' = a \frac{C_0}{C_0'} \quad (9)$$

$$b' = b \frac{C_0}{C_0'} \frac{\ln(C_0' - 1)}{\ln(C_0 - 1)} \quad (10)$$

where b' , b are the new and old intercept, respectively, C_0' and C_0 are the new and old influent concentration, respectively.

2. Materials and methods

2.1. Reagents

All chemicals and reagents used for the study were analytical grades, and all aqueous solutions were prepared in distilled water. Stock solutions of 1,000 mg l⁻¹ MB and 1,000 mg l⁻¹ MO were prepared, while working solutions were obtained by diluting the stock solution. The initial pH of the working solution was adjusted by addition of HNO₃ or NaOH solution.

2.2. Preparation of adsorbent

The raw zeolite used in the study was obtained from Xinyang city in China (purchased from Xinyang's Feedstuff Company). The zeolite was sieved to obtain average size particles about 20–40 mesh and it was immersed in distilled water for 24 h. Then the zeolite was washed by dissolved water and heated at 300°C in muffle furnace for 1 h. After cooled, it was stored for surface coating. The mineralogical composition of zeolite was comprised primarily of clinoptilolite (~68.50%) and additionally of feldspar, montmorillonite and quartz by means of XRD [17].

The process of ICOZ preparation was following: 50 g zeolite and 50 ml ferric chloride solution of 1 mol l⁻¹ were mixed and stirred in two 400 ml glass beaker. The mixture was kept at 80 °C using water bath and 50 ml sodium hydroxide solution (3 mol l⁻¹) was slowly dropped into the mixture with slight stirring. Then the mixture was transferred to evaporating dish, placed in muffle furnace and keeping at 500 °C for 4 h after reaction. The mixture was cooled to room temperature and washed to pH 7.0 using distilled water. Last, the sample was dried at 110 °C, and stored in polypropylene bottle for use.

Elemental identifications of surface features were performed by semi-quantitative EDAX analysis. The EDAX results are following: there are O (48.10%), Mg (0.52%), Al (6.21%), Si (40.21%), K (3.29%), Ca (0.20%), Fe (1.47%) in surface of zeolite by EDAX analysis, while O (22.56%), Cl (9.45%), Na (3.95%), Si (5.47%), K (3.29%), Ca (1.40%), Fe (47.17%) in surface of IOCZ. EDAX analysis yielded direct evidence for iron oxide coated on the surface of zeolite [17].

2.3. Methods of column adsorption

Column adsorption was operated in 0.95 cm diameter glass column (weighted mass of IOCZ packed in column) at 273 K. The dye solution was pumped from the container to the fixed bed with a peristaltic pump at a specified flow rate. The pH of MB and MO solution was adjusted to 7.0 ± 0.1 and 2.5 ± 0.1, respectively [19]. Samples were collected at regular intervals. The concentration of MB and MO in the effluent was analyzed using a Uv/Vis-3000 spectrophotometer at 668 nm and 508 nm, respectively. The mass of 2 cm depth of ICOZ is of 1 g.

3. Result and discussion

3.1. Influence of operating conditions on column sorption of MB and MO

3.1.1. Effect of flow rate

The breakthrough curves at various flow rates of MB and MO were shown in Fig. 1, respectively. From the Fig. 1, it was seen that adsorption arrived saturation faster with increasing flow rate. This tendency accorded with other research [11,17]. At higher flow rate, the external film mass resistance at the surface of the adsorbent tends to decrease and the residence time of the effluent inside the column decreases, hence the time required to reach saturation decrease, furthermore the removal efficiency become lower.

3.1.2. Effect of initial concentration

The change in the initial MB and MO concentration had a significant effect on breakthrough curve (Fig. 2). The larger the initial feed concentration, the steeper is the slope of breakthrough curve and smaller is the breakthrough time. Higher initial influent concentration leads to higher mass transfer driving force, hence more quickly adsorbent saturated, which results in decreasing exhaust time.

3.1.3. Effect of bed depth

The breakthrough curves at various bed depths were shown in Fig. 3. From Fig. 3, as the bed height (adsorbent mass) increased, dye had more time to contact with IOCZ and this resulted in higher removal efficiency of dye molecules in column. So the higher bed column resulted in a decrease in the effluent concentration at the same service time. This was due to an increase in the surface area of adsorbent, which provided more binding sites for adsorption.

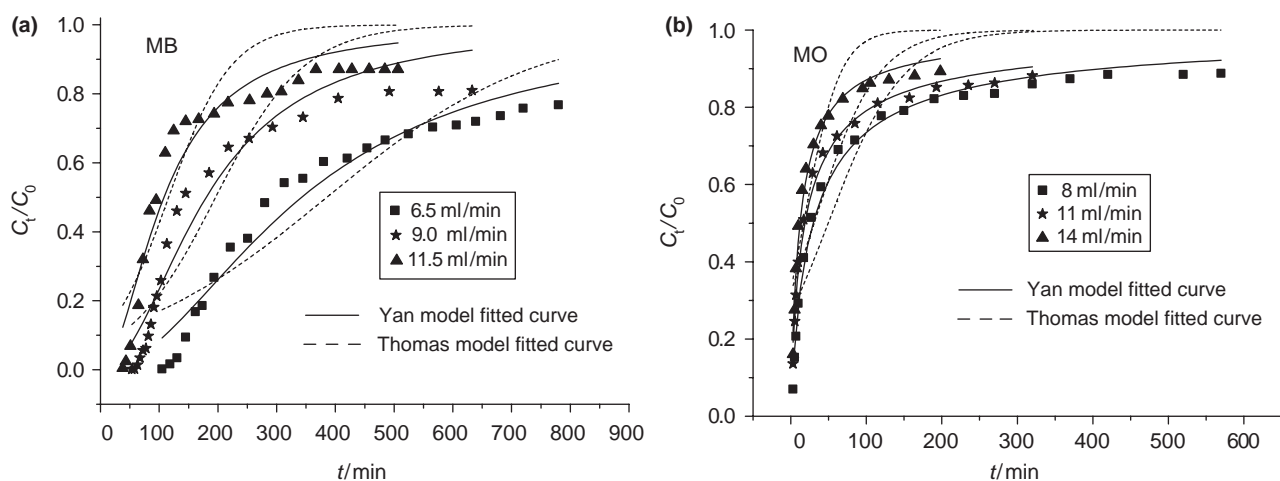


Fig. 1. Experimental and predicted breakthrough curves of dye adsorption at different flow rates: (a) MB ($Z = 16$ cm, $C_0 = 40$ mg l^{-1}); and (b) MO ($Z = 11$ cm, $C_0 = 30$ mg l^{-1}).

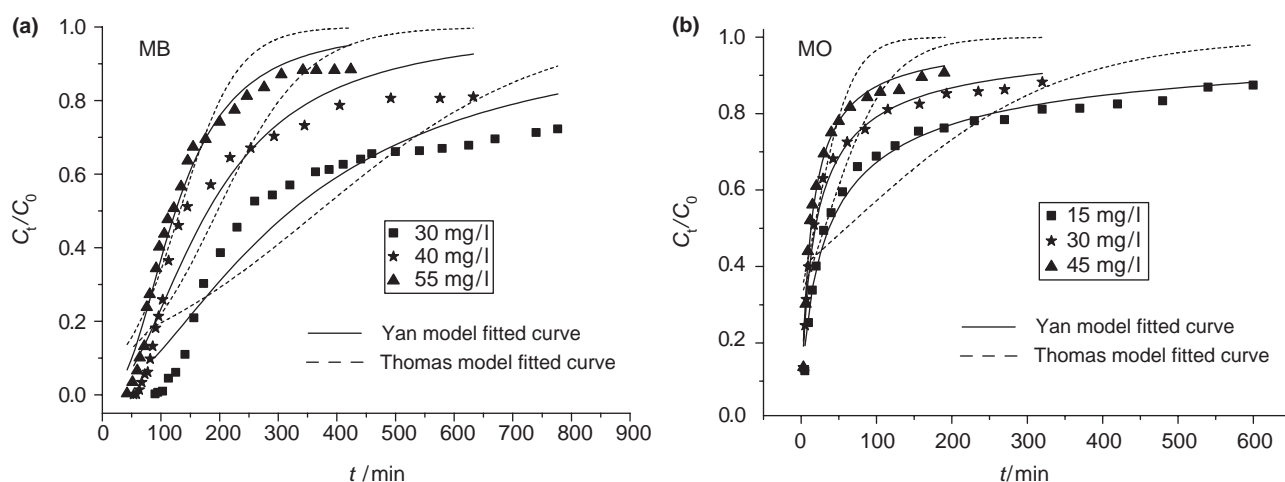


Fig. 2. Experimental and predicted breakthrough curves of dye adsorption at different initial concentrations: (a) MB ($Z = 16$ cm, $Q = 9$ ml min^{-1}); and (b) MO ($Z = 11$ cm, $Q = 11$ ml min^{-1}).

3.2. Evaluation of breakthrough curves

3.2.1. Thomas model

The Thomas model was fitted to investigate the breakthrough behavior of MB and MO onto IOCZ, respectively. The Thomas rate constant (k_{Th}) and value of q_0 were obtained using nonlinear regression analysis according Eq. (1) and the results were listed in Table 1. Analysis of the regression coefficients indicated that the regressed lines provided good fit to the experimental data with R^2 values ranging from 0.74 to 0.92, which were higher relative to more than 20 experimental points. As shown in Table 1, with the bed depth increasing, the values of q_0 increased while k_{Th} decreased, whereas when the flow rate increased, the values of q_0

decreased and the k_{Th} increased. Both of the two parameters changed irregularly with the increase of initial feed concentration.

From Table 1, there were significantly different about the value of q_0 for MB and MO. The adsorption capacity of adsorbent was due to the surface properties of adsorbent, the structures of dyes and experimental conditions [23–25]. The iso-electric point (IEP) of ICOZ in solution is near pH 6.5 [19]. MO was existed as negative ion in solution while MB was positive ion. The surface of IOCZ is positive at pH of solution below IEP. But at pH of solution over IEP, it is negative. So the pH solution of pH in experiment was adjusted to 2.5 for MO while it was not adjusted for MB as the solution of MB is near pH 7.0. Furthermore, it can be implies that the resultant

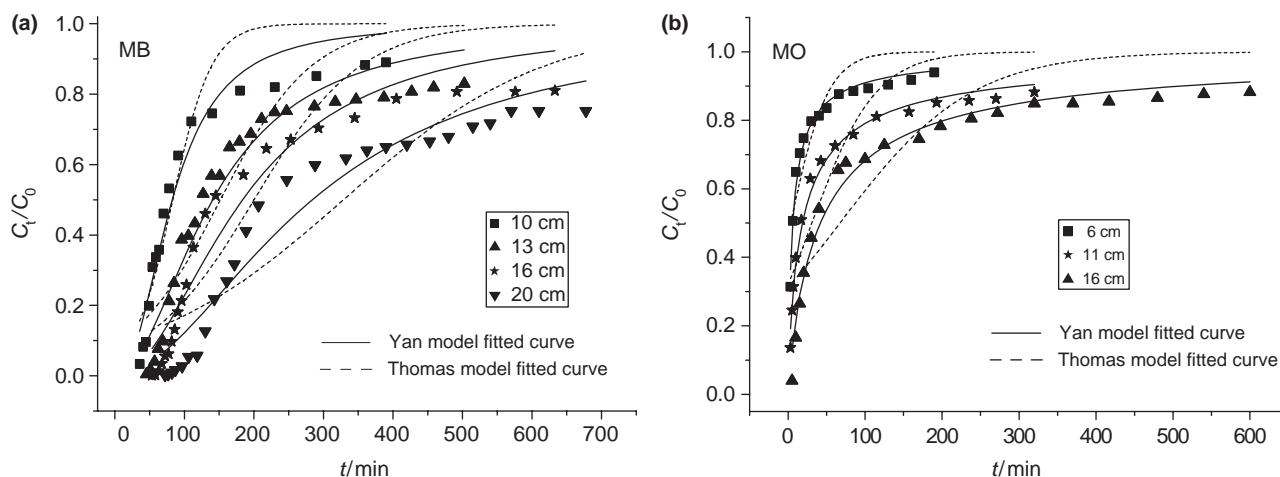


Fig. 3. Experimental and predicted breakthrough curves of dye adsorption at different bed depths: (a) MB ($Q = 9 \text{ ml min}^{-1}$, $C_0 = 40 \text{ mg l}^{-1}$); and (b) MO ($Q = 11 \text{ ml min}^{-1}$, $C_0 = 30 \text{ mg l}^{-1}$).

Table 1

Thomas parameters at different conditions using nonlinear regression analysis

Dye	C_0 (mg l ⁻¹)	Q (ml min ⁻¹)	Z (cm)	$q_{0(\text{cal})}$ (mg g ⁻¹)	k_{Th} (ml (min mg) ⁻¹)	R^2	SSE
MB	40	9	10	5.98 ± 1.04	0.891 ± 0.177	0.880	0.01185
	40	9	13	8.41 ± 1.52	0.381 ± 0.060	0.824	0.0152
	40	9	16	8.83 ± 1.33	0.331 ± 0.059	0.826	0.0178
	40	9	20	11.86 ± 1.53	0.172 ± 0.022	0.834	0.0148
	40	6.5	16	12.52 ± 1.59	0.139 ± 0.017	0.853	0.0109
	40	11.5	16	7.56 ± 1.62	0.401 ± 0.097	0.805	0.0181
	30	9	16	12.50 ± 2.02	0.174 ± 0.028	0.754	0.01835
MO	55	9	16	8.19 ± 0.95	0.372 ± 0.046	0.914	0.00844
	30	11	6	0.334 ± 0.062	1.36 ± 0.35	0.772	0.00785
	30	11	11	1.86 ± 0.62	0.796 ± 0.087	0.786	0.01445
	30	11	16	2.77 ± 0.85	0.391 ± 0.087	0.758	0.01682
	30	8	11	2.16 ± 0.56	0.675 ± 0.156	0.804	0.01596
	30	14	11	1.28 ± 0.44	1.42 ± 0.34	0.804	0.01184
	15	11	11	1.78 ± 0.76	0.476 ± 0.097	0.738	0.0132
	45	11	11	1.56 ± 0.53	0.899 ± 0.210	0.807	0.01123

electrostatic forces mainly determine the adsorption because of pH effect.

Figs. 1–3 also showed the predicted curves using Thomas model at various conditions. It was clear from Fig. 1–3 that there was a good agreement between the experimental points and predicted normalized concentration. Similar results were found by other researches [12,20,26,27].

3.2.2. MDR model

MDR model was fitted to the experimental data of MB and MO at different conditions, respectively. The model constants (a and b) and values of q_0 were given in Table 2. From Table 2, all were fitted with higher

determined coefficients (R^2) ranging from 0.903 to 0.990 and lower values of SSE (less than 0.003). The breakthrough curves predicted by MDR model were also shown in Figs. 1–3.

At all conditions examined, the predicted breakthrough curves from MDR model showed reasonably better agreement with the experimental points than those from Thomas model. It was also shown that the values of q_0 in Table 2 were smaller than those in Table 1, respectively. The trend of values of q_0 and b in Table 2 was similar to values of q_0 in Table 1 with the change of experimental condition. At the lower and high time of breakthrough curves, the fitted curves of Thomas models were far from experimental points. So MDR model was better to predict the MB and MO column

Table 2
MDR parameters at different conditions using nonlinear regression analysis

Dye	C_0 (mg l ⁻¹)	Q (ml min ⁻¹)	Z (cm)	a	b (ml)	$q_{0(\text{cal})}$ (mg g ⁻¹)	R^2	SSE
MB	40	9	10	2.30 ± 0.25	741.2 ± 33.4	5.93 ± 0.27	0.948	0.00515
	40	9	13	1.98 ± 0.16	1,266.4 ± 49.3	7.79 ± 0.30	0.941	0.00512
	40	9	16	2.02 ± 0.19	1,620.5 ± 91.5	8.10 ± 0.46	0.927	0.00742
	40	9	20	1.89 ± 0.15	2,555.7 ± 106.6	10.22 ± 0.42	0.941	0.00525
	40	6.5	16	1.93 ± 0.13	2,227.3 ± 72.4	11.14 ± 0.36	0.955	0.00336
	40	11.5	16	1.87 ± 0.18	1,243.4 ± 66.9	6.22 ± 0.33	0.928	0.00666
	30	9	16	1.70 ± 0.17	2,892.3 ± 148.5	10.85 ± 0.56	0.903	0.00729
	55	9	16	2.42 ± 0.13	1,123.0 ± 25.6	7.72 ± 0.18	0.977	0.00227
MO	30	11	6	0.816 ± 0.039	65.2 ± 4.2	0.652 ± 0.042	0.983	0.00059
	30	11	11	0.790 ± 0.032	203.9 ± 10.6	1.11 ± 0.06	0.989	0.00077
	30	11	16	0.879 ± 0.045	460.6 ± 28.1	1.73 ± 0.11	0.978	0.00154
	30	8	11	0.832 ± 0.030	234.9 ± 11.5	1.28 ± 0.06	0.990	0.00081
	30	14	11	0.903 ± 0.042	169.7 ± 8.1	0.926 ± 0.044	0.985	0.00090
	15	11	11	0.718 ± 0.026	404.0 ± 19.3	1.10 ± 0.05	0.987	0.00069
	45	11	11	0.932 ± 0.043	141.8 ± 6.7	1.16 ± 0.05	0.986	0.00082

Table 3
Calculated constants of BDST model for the adsorption of MB ($C_0 = 40$ mg l⁻¹, $Q = 9$ ml min⁻¹) and MO ($C_0 = 30$ mg l⁻¹, $Q = 11$ ml min⁻¹)

Dye	C_t/C_0	A (min cm ⁻¹)	B (min)	K_a (l (mg min ⁻¹))	N_0 (mg l ⁻¹)	R
MB	0.2	8.90	41.2	0.000842	3,202	0.991
	0.4	11.6	50.0	0.000203	4,173	0.989
	0.6	19.9	110	9×10^{-5}	7,182	0.997
MO	0.2	1.02	5.07	0.00911	337	0.953
	0.4	2.09	9.75	0.001386	691	0.963
	0.6	4.64	21.1	0.00064	1,531	0.988

adsorption than Thomas model. Other researches have published similar results [12,21,27,28].

3.2.3 BDST model

The BDST model was used to evaluate the feasibility of the design of adsorption column for changed flow rate and initial concentration. According to Eqs. (5), (6), the value of related parameters of BDST at C_t/C_0 0.2, 0.4 and 0.6 were shown in Table 3, respectively. With

the increased C_t/C_0 , the values of N_0 increased while K_a decreased. The values of R^2 indicated the validity of BDST model for present system. From Table 2, higher value of N_0 for MB and MO also showed that the ability of MB adsorption on IOCZ was bigger than MO adsorption. According to BDST parameters listed in Table 3, the predicted time (t_c) and experimental time (t_e) at other conditions were shown in Table 4. It was evident from the Table 4 that the calculated time and experimental time were well consistent with each other. So the BDST model can be used to predict adsorption performance at other operating conditions for adsorption of MB and MO onto IOCZ, respectively. Similar results are obtained by other studies [17,22,29,30].

The results also implied that ICOZ, as adsorbent like iron oxide, can effectively remove pollutants with positive charge from solution. For pollutants with negative charge, it may not be available.

4. Conclusions

On the basis of the experimental results of this investigation, the following conclusions can be drawn:

Table 4
Predicted breakthrough time based on the BDST constants for a new flow rate and a new influent concentration

Dye	C_t/C_0	Z (cm)	V' (ml min ⁻¹)	t_c (min)	t_e (min)	C_0' (mg l ⁻¹)	t_c (min)	t_e (min)
MB	0.20	16	11.5	65.6	65.3	55	71.0	74.2
	0.40	16	11.5	89.1	78.7	55	95.3	97.0
	0.60	16	11.5	129	107	55	144	139
MO	0.20	11	14	3.77	3.69	45	3.70	4.15
	0.40	11	14	8.35	7.47	45	8.05	8.13
	0.60	11	14	19.0	16.3	45	18.2	18.9

1. IOCZ was an effective adsorbent for removal of MB and MO from aqueous solution and had larger capacity of MB adsorption.
2. The adsorption of dye was strongly dependent on the flow rate, the initial dye concentration and bed depth.
3. The working stage of breakthrough was described better by MDR model than by Thomas model.
4. BDST model adequately described the adsorption of MB and MO onto IOCZ in column mode.

Acknowledgment

This work was supported by the Natural Science Foundation of Henan Province (92300410030) and the Foundation of Education Department of Henan Province in China (200510459016). Authors thank the referees and editor for giving me valuable comments to improve the quality.

References

- [1] E. Forgacs, T. Cserhati and G. Oros, Removal of synthetic dyes from wastewaters: a review, *Environ. Int.*, 30 (2004) 953–971.
- [2] E. Khan, M. Li and C.P. Huang, Hazardous waste treatment technologies, *Water Environ. Res.*, 80 (2008) 1,654–1,708.
- [3] T. Robinson, G. McMullan, R. Marchant and P. Nigam, Remediation of dyes in textile effluent: a critical review on current treatment technologies with a proposed alternative, *Bioresource Technol.*, 77 (2001) 247–255.
- [4] V.K. Gupta and Suhas, Application of low cost adsorbents for dye removal - A review, *J. Environ. Manag.*, 90 (2009) 2313–2342.
- [5] A.K. Jain, V.K. Gupta, A. Bhatnagar and Suhas, Utilization of industrial waste products as adsorbents for the removal of dyes, *J. Hazard. Mater.*, 101 (2003) 31–42.
- [6] V.K. Gupta and I. Ali, Removal of Endosulfan and Methoxychlor from Water on Carbon Slurry, *Environ. Sci. Technol.*, 42 (2008) 766–770.
- [7] J. Youngran, M.H. Fan, J. Van Leeuwen and J.F. Belczyk, Effect of competing solutes on arsenic(V) adsorption using iron and aluminum oxides, *J. Environ. Sci.*, 19 (2007) 910–919.
- [8] A. Kornmuller, S. Karcher and M. Jekel, Adsorption of reactive dyes to granulated iron hydroxide and its oxidative regeneration, *Water Sci. Technol.*, 46 (2002) 43–50.
- [9] M.K. Doula, Removal of Mn²⁺ ions from drinking water by using Clinoptilolite and a Clinoptilolite-Fe oxide system, *Water Res.*, 40 (2006) 3,167–3,176.
- [10] Y. Xu and I. Axe, Synthesis and characterization of iron oxide-coated silica and its effect on metal adsorption, *J. Colloid Interface Sci.*, 282 (2005) 11–19.
- [11] S. Kundu and A.K. Gupta, Analysis and modeling of fixed bed column operations on As(V) removal by adsorption onto iron oxide-coated cement (IOCC), *J. Colloid Interf. Sci.*, 290 (2005) 52–60.
- [12] X.L. Wu, Y. Wang, J.L. Liu, J.Y. Ma and R.P. Han, Study of malachite green adsorption onto natural zeolite in fixed-bed column, *Desalination Water Treat.*, (2010), doi: 10.5004/dwt.2010.1212.
- [13] D.A. Fungaro, M. Bruno and L.C. Grosche, Adsorption and kinetic studies of methylene blue on zeolite synthesized from fly ash, *Desalination Water Treat.*, 2 (2009) 231–239.
- [14] S.B. Wang and E. Ariyanto, Competitive adsorption of malachite green and Pb ions on natural zeolite, *J. Colloid Interface Sci.*, 314 (2007) 25–31.
- [15] R.P. Han, Y. Wang, W.H. Zou, Y.F. Wang and J. Shi, Comparison of linear and nonlinear analysis in estimating the Thomas model parameters for methylene blue adsorption onto natural zeolite in fixed bed column, *J. Hazard. Mater.*, 145 (2007) 331–335.
- [16] R.P. Han, Y. Wang, Q. Sun, L.L. Wang, J.Y. Song, X.T. He and C.C. Dou, Malachite green adsorption onto natural zeolite and reuse by microwave irradiation, *J. Hazard. Mater.*, 175 (2010) 1,056–1,061.
- [17] R.P. Han, L.N. Zou, X. Zhao, Y.F. Xu, Y.F. Li, Y.L. Li and Y. Wang, Characterization and properties of iron oxide-coated zeolite as adsorbent for removal of copper (II) from solution in fixed bed column, *Chem. Eng. J.*, 149 (2009) 123–131.
- [18] L.N. Zou, Y.F. Xu, X.H. Ma, J.Y. Ma and R.P. Han, Adsorption of methylene blue and copper ions from aqueous solutions by iron-oxide-coated-zeolite, *J. Zhengzhou Uni.(Sci. Ed.)*, 41(3) (2009) 78–84.
- [19] L.N. Zou, Study of adsorption of methylene blue, methyl orange and copper ions from the aqueous solutions by iron-oxide-coated-zeolite, Master thesis of Zhengzhou University, 2009.
- [20] Z. Aksu and F. Gonen, Biosorption of phenol by immobilized activated sludge in a continuous packed bed: prediction of breakthrough curves, *Process Biochem.*, 39 (2004) 599–613.
- [21] G. Yan, T. Viraraghavan and M. Chen, A new model for heavy metal removal in a biosorption column, *Adsorpt. Sci. Technol.*, 19 (2001) 25–43.
- [22] J. Goel, K. Kadirvelu, C. Rajagopal and V.K. Garg, Removal of lead(II) by adsorption using treated granular activated carbon: Batch and column studies, *J. Hazard. Mater.*, 125 (2005) 211–220.
- [23] A. Mittal, J. Mittal, A. Malviya, D. Kaur and V.K. Gupta, Adsorption of hazardous dye crystal violet from wastewater by waste materials, *J. Colloid Interface Sci.*, 343 (2010) 463–473.
- [24] V.K. Gupta, A. Mittal, L. Kurup and J. Mittal, Process development for removal and recovery of Metanil Yellow by adsorption on waste materials—bottom ash and de-oiled soya, *J. Hazard. Mater.*, 151 (2008) 834–845.
- [25] V.K. Gupta, P.J.M. Carrott, M.M.L. Ribeiro Carrott and Suhas, Low cost adsorbents: Growing approach to wastewater treatment - A review, *Crit. Rev. Environ. Sci. Technol.*, 39 (2009) 783–842.
- [26] R.P. Han, Y. Wang, W.H. Zou, Y.F. Wang and J. Shi, Comparison of linear and nonlinear analysis in estimating the Thomas model parameters for methylene blue adsorption onto natural zeolite in fixed-bed column, *J. Hazard. Mater.*, 145 (2007) 331–335.
- [27] K. Vijayaraghavan and D. Prabu, Potential of *Sargassum wightii* biomass for copper(II) removal from aqueous solutions: Application of different mathematical models to batch and continuous biosorption data, *J. Hazard. Mater.*, 137 (2006) 558–564.
- [28] P. Lodeiro, R. Herrero and M.E. Sastre de Vicente, The use of protonated *Sargassum muticum* as biosorbent for cadmium removal in a fixed-bed column, *J. Hazard. Mater.*, 137 (2006) 244–253.
- [29] R.P. Han, Y. Wang, X. Zhao, Y.F. Wang, F.L. Xie, J.M. Cheng and M.S. Tang, Adsorption of methylene blue by phoenix tree leaf powder in a fixed-bed column: experiments and prediction of breakthrough curves, *Desalination* 245 (2009) 284–297.
- [30] R.P. Han, D.D. Ding, Y.F. Xu, W.H. Zou, Y.F. Wang, Y.F. Li and L.N. Zou, Use of rice husk for the adsorption of congo red from aqueous solution in column mode, *Bioresource Technol.*, 99 (2008) 2,938–2,946.